Higher symmetries for electromagnetic devices

O. Quevedo-Teruel, *Senior Member, IEEE,* G. Valerio, *Senior Member, IEEE,* Z. Sipus, *Senior Member, IEEE,* and E. Rajo-Iglesias, *Senior Member, IEEE,*

HIGHER SYMMETRIES have frequently amazed human beings because of the illusions and incredible landscapes that they can produce. For example, we can think in the unearthly pictures of the Dutch graphic artist Maurits Cornelis Escher. He made use of glide symmetry to produce unbelievable transitions and transformations of objects and beings inspired in glide reflections, as illustrated in Fig. 1 (a). However, the history of higher symmetries started much earlier in time. M. C. Escher got part of his inspiration in the Moorish tessellations in the Alhambra of Granada, Spain, as the ones illustrated in Fig. 1 (b). Higher symmetries cannot only be employed to create artistic creations, but also to enhance the performance of electromagnetic devices. Here, we will explain the importance of the recently discovered electromagnetic properties of higher symmetries, as well as their implications and opportunities for microwave and antenna engineers.

I. HIGHER SYMMETRIES IN THE ELECTROMAGNETIC HISTORY: BACK TO THE 60S

When narrowing our scope to Physics, higher symmetries were very popular in the 60s. For example, George L. Trigg wrote in 1965 that "in the last few months, scarcely an issue of Physical Review Letters has failed to contain at least one paper on the topic" [1], demonstrating the volume of studies in this topic. If we are more specific, and we focus our attention to electromagnetic engineering, the first studies on higher symmetries arrived in the middle of the 60s [2], [3], and they were popular for one decade, until the middle of the 70s [4], [5]. However, in the 70s, the electromagnetic engineering community was not ready to further develop scientific studies on higher symmetries and to understand their full potential. First of all, computers were very basic and there was no commercial software that could be used to simulate these complex structures. Second, the understanding of periodic structures achieved its maturity in the 2000s with the arrival of the concept of metamaterials. Finally, at the end of the 70s and beginning of the 80s, the electromagnetic engineers focused their attention in making wireless systems affordable for everybody, so printed and planar technology was the selected solution for low-cost communications at low frequencies.

It was in the second decade of the 21st century, when powerful computers became easily accessible, commercial software of simulation is commonly available, and periodic structures are broadly understood thanks to the studies on metamaterials, when the opportunity for higher symmetries has arrived. This opportunity came when the industry demanded electromagnetic systems operating at higher frequencies. At these frequency ranges, there is a need for low-loss structures that can only be achieved with fully-metallic devices and integrated systems such antennas and circuits.

In this situation, antennas based on leaky waves and lenses are gaining adepts for communications designs in the new bands of 5G and satellite communications [6]. Although the design of these antennas is more complicated than arrays, they present a
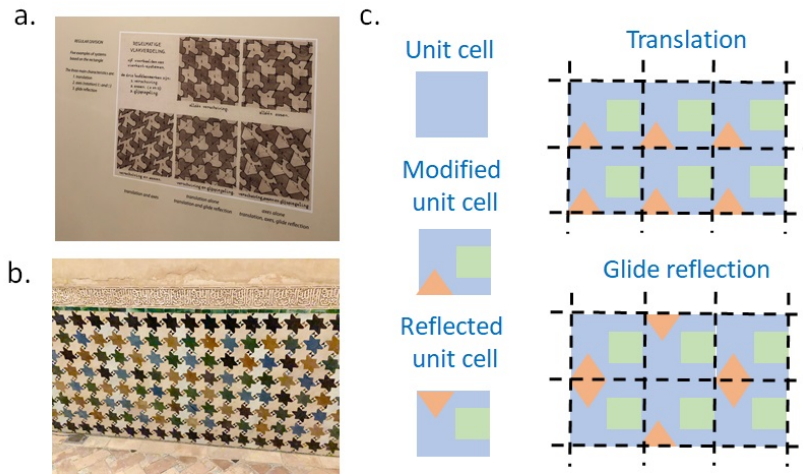
Fig. 1. Glide symmetries in art: a) Explanation of glide reflection at the museum of M. C. Escher in The Hague, The Netherlands. b) Moorish tessellations in the Alhambra of Granada, Spain. c) Compositions made of translations and glide reflection.

more simple feeding network. On the other hand, filters were traditionally designed as an independent unit that was connected to the rest of the system. Due to the insertion losses, and the losses in the interconnections, for high-frequency designs, they must be integrated together with other components. Finally, due to the large losses, future components, such as filters, must be reduced in length. Therefore, design techniques which are not based on isolated elements, but in coupled elements, are required to reduce the overall losses.

II. DEFINITION OF HIGHER SYMMETRIES

A periodic unit cell possesses higher symmetries when it is invariant after a translation and a second geometrical variation. For example, a glide-symmetric unit cell is invariant after a translation and a mirroring [5]. A twist-symmetric unit cell is invariant after a translation a rotation or angular movement [7].

A. Glide symmetries

In Fig. 1 (c), we represent the creation of a periodic structure trough a glide-reflection. A unit cell, represented in blue, is filled with with a triangle and a rectangle. One could repeat this unit cell with a simple translation, but also, create a reflected unit cell that is alternated together with the translation.

When speaking about glide symmetries, we can identify one-dimensional and two-dimensional configurations. In Fig. 2 (a,b), we represent two examples of one-dimensional glide-symmetric structures: corrugations [8], [9], [10] and transversal slots [11], [12]. These two structures have glide symmetry with respect to the direction, however their mirroring planes are different. In the corrugations, this plane is horizontal, but in the slots, it is vertical. In these cases, the glide operation is $\rightarrow + 2$, and either $\rightarrow -$ in the corrugations, or $\rightarrow -$ in the slot, with as periodicity in both cases.

A new particular case of glide symmetry was recently reported as polar glide symmetry [7], [13]. It refers to the case in which the mirroring plane is not defined with Cartesian coordinates, but with polar ones. Therefore, the mirroring plane is orthogonal to a vector in direction [13], [14].
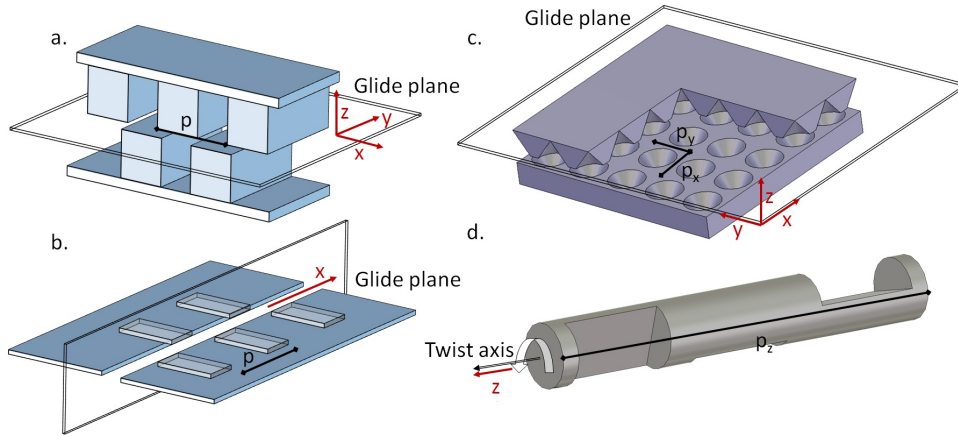
Fig. 2. Electromagnetic configurations of higher symmetries: a) Glide-symmetric corrugations. b) Slot with glide-symmetric transversal loads. c) Two dimensional glide-symmetric holey structure. d) Twist-symmetric holey configuration.

Two dimensional glide-symmetric structures were first studied in [15], and they require the translation in two orthogonal directions that are opposite to the vector of the mirroring plane. For example, a common glide operation can be ( ) → (+ ₓ 2 + ᵧ 2) and → − [16], [17], with as periodicity. One example of two-dimensional glide symmetry is shown in Fig. 2 (c) for conical holes in a metallic parallel plate.

B. Twist symmetries

Twist-symmetric structures are those invariant under a translation in one direction. For example, in Fig. 2 (d) a holey metallic wire oriented in direction is illustrated. This direction is the propagation direction. The wire has holes that rotate through direction. A periodic structure possess a -fold twist symmetry, being an integer, if it is invariant under a translation along and 2 rotation around the twist direction, where is the periodicity of the structure [13]. The particular case shown in Fig. 2 (d) is 3-fold. We must note that helices are a particular case of twist symmetry with = ∞. These helices were studied in terms of dispersion properties in the 50s [18]. Therefore, twist symmetry is also known as helical symmetry or screw symmetry [5].

III. SUB-PERIODICITIES IN HIGHER SYMMETRIES

Introducing higher symmetries in periodic structures may drastically change the dispersion properties of those structures, i.e. how pass-bands and stop-bands are distributed in the frequency domain. The basic property of higher-symmetric periodic structures is the possibility to close selected band-gaps. This was already discussed by Hessel *et al.* [5] in the early 70s, with reference to 1-D structures. Specifically, the presence of a glide symmetry with period closes the first stop-band at the edge of a Brillouin zone (= , being the phase constant of a Bloch mode), and a -fold twist symmetry closes the first − 1 stop-bands, alternatively at = and = 0. The same spectral properties have been more recently observed in 2-D structures.

For example, in a glide-symmetric structure, the absence of a stop-band at = can be simply explained if the effect of the periodic scatterers on the two sides of the glide plane is the same. This means that these scatterers can be moved on the same side of the plane, thus transforming the glide structure into an equivalent purely periodic structure with a *halved spatial*
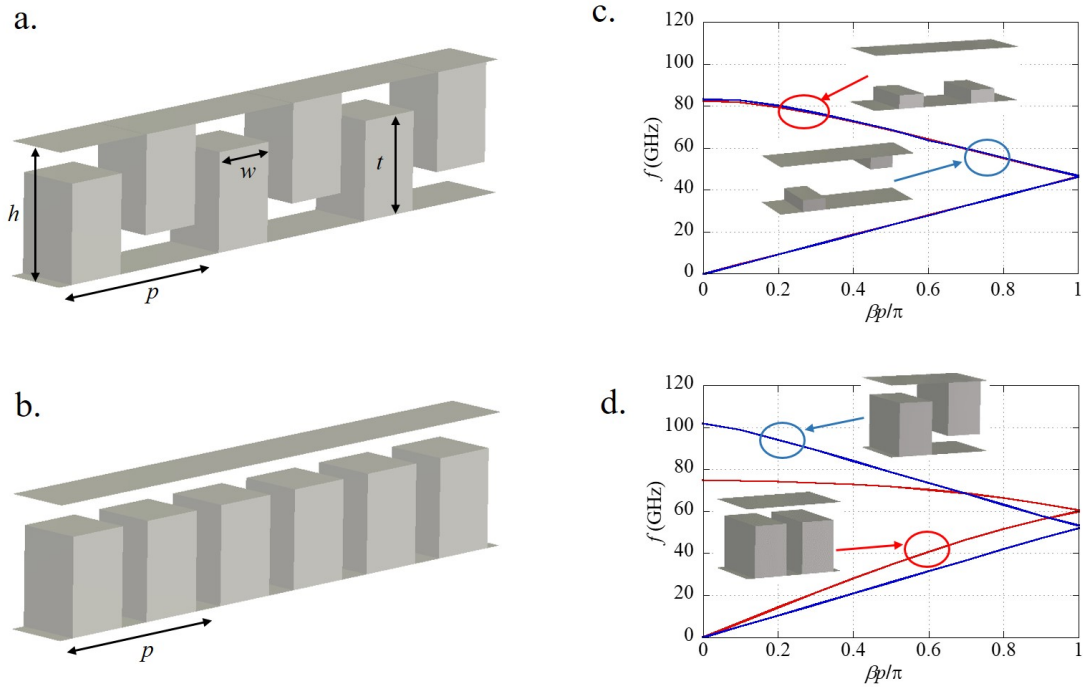
Fig. 3. a) Structure with glide-symmetric corrugations along one direction. b) Associated non-glide-symmetric structure with corrugations along one direction. (c) Brillouin diagram of glide and non-glide structures with $h = 1$ mm, $w = 0.5$ mm, $p = 3$ mm and $t = 0.25$ mm. d) Brillouin diagram of glide and non-glide structures with $h = 1$ mm, $w = 0.5$ mm, $p = 1.5$ mm and $t = 0.75$ mm.

period 2. One example of one-dimensional glide structure and its associated non-glide are depicted in Figs. 3 (a) and (b). The Brillouin diagram of this new non-glide periodic structure presents a first stop-band edge at $ = (2) = 2 $, which is equivalent to the $ = 0$ point in the diagram of the glide structure. In other words, the glide structure is equivalent to a structure with a shorter period, so that its first stop band is found at a higher frequencies.

However, the equivalence between scatterers on the two sides of the glide plane is not necessarily verified in all glide structures. In order to explain this phenomenon, let us decompose the Bloch mode supported by the glide structure into the modes of the uniform background structure. These modes are coupled together by the periodic scatterers. In the glide structure of Fig. 3 (a) these scatterers are placed alternatively on the two sides of the glide plane, while in the periodic structure of Figs. 3 (b) they are all on the same side.

On one hand, if in both structures the scatterers are *weakly interacting* among each other, only one dominant mode is relevant in the coupling between adjacent scatterers. This happens if each scatterer mainly excites only one dominant background mode, or if all the background modes excited by one scatterer are strongly attenuated when they reach the adjacent ones. In this case, the mutual position of two adjacent scatterers does not impact the coupling, which is the same whether both scatterers lie on the same side of the glide plane or on opposite sides of it. The glide structure is then *reducible* to the non-glide periodic structure with halved spatial period [19]. An example of reducible glide structure can be seen in Fig. 3 (c), where the glide line and the non-glide line have the same dispersion diagram, if their phase constants are normalized with respect to the same distance (the period of the glide line). On the other hand, if at least in one of the two structures of Figs. 3 (a) and (b) the scatterers are *strongly interacting* among them, several background modes will be relevant for their coupling [20]. These modes

will have in general different parity with respect to the glide plane; the odd and the even modes will experience a different scattering according to the position of the scatterer with respect to the glide plane. This richer modal coupling in strongly coupled structures makes the glide-symmetric one *irreducible* to the non-glide periodic one with reduced spatial period [19]. An example of irreducible glide structure can be seen in Fig. 3 (d), where the glide line and the non-glide line have different dispersion diagrams. The same phenomena can be found in twisted structures, where the scatterers lie along a spiral, rather than on different sides of a plane [21]. This will be explained in detail in Section VIII.

IV. CIRCUIT MODELS TO ANALYZE GLIDE-SYMMETRIC STRUCTURES

Due to the recent interest in higher-symmetric structures, simplified models for the simple design of these structures are not yet available. The need for specific models of higher symmetric structures is due to the difficult application of many full-wave numerical methods to this class of structures. Interesting dispersive behaviors, such as wideband response and strong band-gap rejection, require extreme values of geometrical parameters (e.g., very close glide surfaces in order to enhance their mutual interaction). In these cases, numerical methods encounter difficulties: for example, thin gaps between surfaces require a very dense localized meshing in finite-element and finite-difference methods, or cause slow convergence in Green's functions in the method of moments. Furthermore, the study of finite structures made by a non-uniform array of thousands of sub-wavelength cells is a multiscale problem whose solution requires *ad-hoc* computation techniques.

A. Circuit models

In this framework, the availability of equivalent circuits for the unit cells of higher-symmetric structures of interest would considerably simplify their preliminary design. Based on the previous analysis, if a higher-symmetric structure is reducible to a non higher-symmetric periodic structure, a mono-modal equivalent circuit is sufficiently accurate to calculate its dispersion behavior. Furthermore, the model can be performed only on a sub-unit cell, and the non higher-symmetric structure can be analyzed instead of the higher-symmetric structure. This was done in [9], where a one-dimensional glide-symmetric corrugated structure was analyzed by means of an equivalent circuit derived by the T-junction discontinuity [22]. Results of this equivalent circuit are extremely accurate for all range of parameters used in the current applications. More recently, a circuit model analysis was proposed to model glide-symmetric loaded microstrip lines [23]. This model accurately explains the coupling effects between unit cells, and the different interaction between conventional and glide-symmetric unit cells.

B. Multi-mode analysis

When irreducible structures are of interest, a multi-modal equivalent circuit can always be used in order to correctly model the interactions among the different scatterers [19], [21]. In a one-dimensional higher-symmetric line, the unit cell can then be modeled as a 2 -port network, where is the number of background modes retained on each Floquet boundary of the cell in order to accurately compute the interactions between scatterers. This network can be characterized by means of its transmission matrix $\boldsymbol{T}$, whose eigenvalues are related to the wavenumbers of the Bloch modes supported by the structure. If only two modes are relevant, we get:

$$\boldsymbol{T} \cdot \begin{bmatrix} V^{(1)} \\ V^{(2)} \\ I^{(1)} \\ I^{(2)} \end{bmatrix} = e^{\jmath k_z p} \begin{bmatrix} V^{(1)} \\ V^{(2)} \\ I^{(1)} \\ I^{(2)} \end{bmatrix} \tag{1}$$

where $V^{(1)}$ and $I^{(1)}$ are the voltage and currents associated to the first mode on one Floquet boundary of the cell, $V^{(2)}$ and $I^{(2)}$ are the voltage and currents associated to the second mode on the same Floquet boundary, and k_z is the (possibly complex) unknown Bloch wavenumber. Its real part, β, is the phase constant of the Bloch mode and its imaginary part, α if present, is its attenuation constant.

This description in terms of transmission matrix can also lead to an alternative approach to perform a dispersion equation, by means of the multi-modal transmission matrix of a sub-cell. In this case, we need to take into account that after translating one sub-cell, each background mode composing the Bloch mode is not equivalent to a phase shift (as a translation of one cell is). In order to get a phase shift, we need to perform also a reflection [19] or rotation [21], according to the glide or twisted nature of the structure. We can compensate each background mode for this geometrical operation by multiplying each mode by a factor depending on the mode parity. In the case of a glide line, if the first mode in (1) is even with respect to the glide plane and the second mode is odd, we get:

$$\boldsymbol{T}_{1/2} \cdot \begin{bmatrix} V^{(1)} \\ V^{(2)} \\ I^{(1)} \\ I^{(2)} \end{bmatrix} = e^{\jmath k_z p/2} \begin{bmatrix} V^{(1)} \\ -V^{(2)} \\ I^{(1)} \\ -I^{(2)} \end{bmatrix} \tag{2}$$

where the transmission matrix $\boldsymbol{T}_{1/2}$ is now referred only to one half of the unit cell (thus requiring a faster computation). Eq. (2) confirms also that the presence of only one mode (or the presence of modes with the same parity) in both (1) and (2) makes the structure equivalent to a non-glide periodic line, having as a unit cell the sub-cell of the glide line. All these results can be easily generalized to two-dimensional glide structures [19], where background modes can be defined on each of the four Floquet boundaries of the unit cell.

V. MODE-MATCHING TO ANALYZE GLIDE-SYMMETRIC STRUCTURES

An appropriate way of analyzing guiding electromagnetic structures having higher symmetries is to apply the mode matching analysis approach. Mode matching is based on representing the electric and magnetic fields in each section of the structure as a sum of suitable modes with unknown complex amplitudes. In other words, it uses the pre-knowledge about the electromagnetic field configuration and symmetry properties to reduce the number of unknowns. With this technique, it possible to describe precisely the electromagnetic fields in the structure and to give a physical insight about the properties of higher symmetries.

A. Fully-metallic glide-symmetric structures

As an example, let us consider a parallel-plate waveguide (PPW) with glide-symmetric holey walls (Figs. 2.a and 2.c). The electromagnetic fields in the PPW region (parallel to the walls) can be expressed as a series of Floquet harmonics by virtue of periodicity:

$$
\begin{aligned}
\mathbf{E}_t^{Gap} &= \frac{1}{d^2}\sum_{p,q} e^{\jmath(k_{x,p}x+k_{y,q}y)}\tilde{\mathbf{e}}_{t,pq}^{Gap}(z)\\
\mathbf{H}_t^{Gap} &= \frac{1}{d^2}\sum_{p,q} e^{\jmath(k_{x,p}x+k_{y,q}y)}\tilde{\mathbf{h}}_{t,pq}^{Gap}(z)
\end{aligned}
\tag{3}
$$

with $k_{x,p}=k_{x,0}+2\pi p/d$ and $k_{y,q}=k_{y,0}+2\pi q/d$ by assuming a rectangular lattice with period d in both x and y directions. The amplitude of each Floquet harmonic of the transverse electric field can be written as

$$
\begin{aligned}
\tilde{\mathbf{e}}_{t,pq}^{Gap}(z) &= \begin{pmatrix} A_{pq}^x \\ A_{pq}^y \end{pmatrix}\sin(k_{z,pq}z)+\begin{pmatrix} B_{pq}^x \\ B_{pq}^y \end{pmatrix}\cos(k_{z,pq}z)\\
\tilde{\mathbf{h}}_{t,pq}^{Gap}(z) &= \begin{pmatrix} D_{pq}^x \\ D_{pq}^y \end{pmatrix}\sin(k_{z,pq}z)+\begin{pmatrix} F_{pq}^x \\ F_{pq}^y \end{pmatrix}\cos(k_{z,pq}z)
\end{aligned}
\tag{4}
$$

where $k_{z,pq}=(k_0^2-k_{x,p}^2-k_{y,q}^2)^{1/2}$ is the vertical wavenumber of the $(p,q)^{th}$ harmonic. This electromagnetic distribution is *matched* to the zero tangential E-field at the metallic parts of the PPW walls and to the tangential electromagnetic field distribution in the lateral waveguides

$$
\begin{aligned}
\mathbf{E}_t^{WG}(z=\tfrac{g}{2}) &= \sum_m r_m C_m \mathbf{\Phi}_m(x,y)\\
\mathbf{H}_t^{WG}(z=\tfrac{g}{2}) &= \sum_m r_m^+ Y_m C_m[\hat{z}\times\mathbf{\Phi}_m(x,y)]
\end{aligned}
\tag{5}
$$

where C_m is the unknown coefficient of the mth mode and $\mathbf{\Phi}_m$ and Y_m are the corresponding cross section modal function and the wave admittance. In the formulation both the E- and H-field components should be matched at the lateral waveguide openings by which it is possible to determine the unknown coefficients. One should note that the selected waveguide modes are orthogonal in PPW and lateral waveguide sections, but they are not mutually orthogonal. Therefore, the bi-Galerkin method is applied (i.e. waveguide modes of the PPW and of the lateral waveguides are used to test the E- and H-field equations), and the mode-matching matrix is densely filled.

The generalized Bloch theorem [5], [16], [17], [24] states that the field repeats itself (apart from an exponential factor) after a translation of half a period and a mirroring operation:

$$
\mathbf{E}(x,y,-z)=\pm e^{\jmath(k_{x,0}\frac{d}{2}+k_{y,0}\frac{d}{2})}\mathbf{E}\left(x-\frac{d}{2},y-\frac{d}{2},z\right)
\tag{6}
$$

The following translation property of the Fourier transformation will give the physical insight of the glide symmetry

$$
\frac{1}{d^2}\int\int\mathbf{\Phi}_m\left(x-\frac{d}{2},y-\frac{d}{2}\right)e^{\jmath(k_{x,0}\frac{d}{2}+k_{y,0}\frac{d}{2})}e^{\jmath(k_{x,p}x+k_{y,q}y)}dxdy=\tilde{\mathbf{\Phi}}_m(k_{x,p},k_{y,q})(-1)^p(-1)^q
\tag{7}
$$

In other words, depending on the index of the Floquet mode, we have even or odd symmetry across the $z=0$ plane; the

presence of glide symmetry causes that the odd and even symmetries are mixed inside the PPW resulting in extraordinary properties of the guiding structure. This can be illustrated if we assume that the field distribution in the lateral waveguides is described with only one waveguide mode. In that case, the linear system (whose determinant represents the characteristic equation of the mode travelling along the glide symmetric periodic structure) is reduced to a single equation

$$\sum_{\substack{p+q \\ \text{even}}} \tilde{\Phi}(k_{x,p}, k_{y,q}) \tilde{\Phi}(-k_{x,p}, -k_{y,q}) \frac{k_0^2 - k_{y,q}^2}{k_{z,pq}} \cot(\frac{k_{z,pq} g}{2})$$

$$- \sum_{\substack{p+q \\ \text{odd}}} \tilde{\Phi}(k_{x,p}, k_{y,q}) \tilde{\Phi}(-k_{x,p}, -k_{y,q}) \frac{k_0^2 - k_{y,q}^2}{k_{z,pq}} \tan(\frac{k_{z,pq} g}{2}) + j d^2 \frac{r^+}{r} k_{z,01}^{WG} = 0 \quad (8)$$

The presence of the glide symmetry causes that for even Floquet mode indices (i.e. for $p + q$ even number) the E-field in the parallel-plate region is described with $\cos(k_{z,pq}z)$ terms (i.e. with terms having even symmetry across the $z = 0$ plane), while for odd Floquet mode indices, the E-field is described with $\sin(k_{z,pq}z)$ terms, i.e. with terms having odd symmetry, see eq. (4).

It is interesting to compare this characteristic equation with the one given for an open holey surface [25]. In the case of open surface there is no mixing of odd and even modes, since there is no second holey surface forming the PPW, i.e. only the outgoing waves are present, so usually it is enough to consider only one PPW mode. The situation is different when a top ground plane approaches to the structure [26], [27] or the structure possesses glide symmetry [16], [17], [24].

B. Dielectric glide-symmetric structures

Till now, most of the realized prototypes possessing higher symmetry were made from metal. However, in many applications and specially when going higher in frequency towards optics, dielectrics are the preferred building material. Although at the first glance there are a lot of similarities between the analysis of metallic and dielectric glide-symmetric structures, the main difference comes from the fact that in the dielectric case part of the propagating wave (and thus part of the electromagnetic power) travels outside the dielectric waveguide. The wave propagating in the corrugated region can be modeled as a wave propagating along a periodic array of dielectric slabs [28], and it has to be matched at both interfaces with the modes present in PPW and in free-space, respectively [29]. For propagation constants smaller than the one of free-space, a fast wave is excited which leads to leakage of electromagnetic energy, i.e. the considered structure actually represents a leaky-wave antenna.

VI. GLIDE-SYMMETRY TO CREATE STOP-BANDS AND EBGs (ELECTROMAGNETIC BAND GAPS)

Some of the recently proposed structures with higher symmetries, and specifically those with glide symmetry, have been studied for their ability to produce stop-bands or band-gaps. Periodic structures have been often used on antenna designs to eliminate surface waves such as the Sievenpiper mushrooms [30]. These periodic structures are used, for example, to reduce the mutual coupling between antennas [31] or to produce filters [32].

On the other hand, a new technology known as gap waveguide was recently proposed for high frequency microwave circuits and antennas [33], [34]. This technology requires stop-bands for parallel plate modes instead of surface waves, i.e. the periodic structure is embedded in a parallel-plate structure. One of the most popular types of gap waveguides is the *groove* gap

waveguide technology [35]. This technology is equivalent to a conventional rectangular waveguide in which the solid lateral walls are replaced by an EBG structure. By using this EBG structure, the manufacturing of the waveguide is made in two pieces that are assembling together afterwards by simply screwing. Electrical contact between the two pieces is not strictly required.

A. Analysis of two-dimensional holey glide-symmetric EBGs

One possible solution to create stop-bands between parallel plates is to use periodic holes, as proposed in [36]. However, the stop-band in all directions (i.e. EBG) created by holey structures is typically narrow, as illustrated in Fig. 4 (a). Even after a thorough optimization of the constituent parameters of the holes, the stop-band is far from the one produced with pin-type structures [37].

In [38], it was demonstrated that holey structures with glide symmetry have a larger EBG bandwidth than conventional periodic holey structures. Indeed, the replacement of the top metal lid for a periodic structure made of holes, as shown in Fig. 4 (a), modifies all the modes propagating in the structure and creates a huge stop-band in between the second and third mode that can be used, for example, for gap waveguide technology [39], [40], [41], [42].
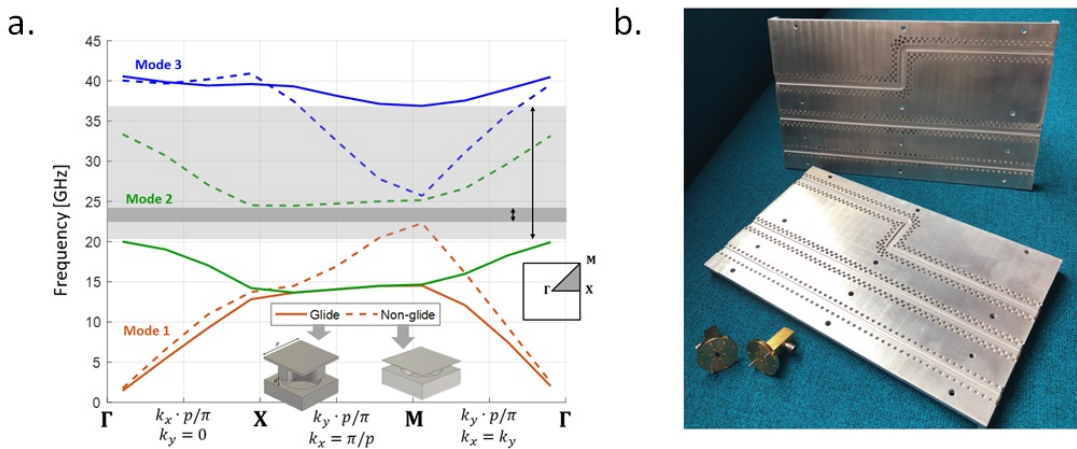

Fig. 4. (a) Comparison of the dispersion diagram for holey structures with and without glide symmetry. (b) Photo of a manufactured groove gap waveguide using a glide-symmetric holes [39] and a glide-symmetric flange [43].

A complete parametric study of the glide-symmetric holey structures in terms of stop-band properties was carried out in [37]. The results on this study can be summarized as follows. First of all, the period of the structure plays a key role in glide-symmetric holey structures since it determines the frequency range of operation. This implies that this periodic structure is electrically larger than those made of pins. Secondly, the ratio between the periodicity and the hole radius defines the bandwidth of the stop-band. There is an optimal ratio, approximately 0.25, that maximizes the bandwidth of the stop-band.

Another relevant conclusion is the fact that the depth of the holes is affecting the behaviour of the structure up to a given height. This has interesting consequences for the manufacturing of the structure, since the depth of the holes does not need to be precisely controlled. In other words, after a given height, the bottom of the hole minimally affects the performance of the EBG. This property can be understood with the mode matching analysis presented in the previous section. Since only

evanescent modes penetrate into the hole, these modes are vanished after a given depth, making this structure practically insensitive to the flatness and height of the hole.

Finally, similarly to other periodic structures such as pin-type, when the gap size is decreased, the stop-band increases, mainly due to the reduction in the cut-off frequency of the first mode.

B. Holey glide-symmetric structures for gap waveguide Technology

One popular application of EBGs is in a parallel plate scenario for its potential use in gap waveguide technology. A number of periodic structures, typically pin-type, corrugations and mushroom-type, have been proposed for gap waveguide technology [44]. This type of waveguide can be also implemented with glide-symmetric holes acting as an EBG [39]. The two main advantages of this implementation are the simplified manufacturing and robustness. The presence of the glide-symmetric holey structure stops the leakage produced by the irregularities on the two surfaces, which are not perfectly attached in practice. With this approach, as is illustrated in the photo of Fig. 4 (b), it is possible to design waveguide components. For example, phase shifters were presented in [40] and [42]. Another example of a component made with this version of the technology is a   to   mode converter, which was used in [45] to produce a transversally compact slot array. Glide symmetry has been also proposed to produce highly-efficient millimetre-wave arrays [46].

Finally, a recent work [41] explored the possibilities of breaking the symmetry of the holes to add filtering capabilities to gap waveguide technology. Recent implementations of glide symmetry make also use of multi-layer structures to reduce the manufacturing cost at high frequency [47].

C. Glide symmetry for flanges

Another interest use of glide symmetry as an EBG was proposed in [43]. In this case, holey glide-symmetric holes were introduced in a waveguide flange to avoid the leakage between connections. This technique can be used to produce fast measurements at very high frequencies since no physical contact between flanges is required. This idea was previously proposed with pins instead of holes in [48]. Here again, the solution with holes is remarkably more robust and simple to manufacture than pin-type. The concept was experimentally validated in the U-band in [43]. The designed flanges in this work are illustrated in the photo of Fig. 4 (b).

D. Controllable stop-bands on planar technology

Although glide symmetry became popular for its immediate application to gap waveguide technology, its opportunities are beyond this specific technology. For example, glide symmetry has been applied to multi-layer dielectric planar technology to reduce the operation frequency of conventional stop-gaps [49].

Glide symmetry has also been applied to transmission lines. For example, it was proposed in CPW (Co-Planar Waveguide) to independently control the stop-bands of even and odd modes [12]. Similarly, glide symmetry was employed in planar bifilar technology to control the stop-bands generated by creating or breaking this symmetry [50].

In [23], it was demonstrated that using glide-symmetric mushrooms, the bandwidth of a stop-band in microstrip technology can be increased without adding any extra cost of manufacturing. Finally, in [51], elliptical holes between two dielectric layers

were proposed to produce stop-bands by breaking the glide symmetry. In this work, it was demonstrated that the width of these stop-bands and their attenuation depends on the level of symmetry that is broken.

VII. GLIDE SYMMETRIES TO REDUCE THE DISPERSION

Another important feature of higher symmetries, and in particular of glide symmetry, is that they may be used to reduce the dispersion of the first propagating mode in a periodic structure. This phenomenology has been used to create broadband lenses and low-dispersive transmission lines that find application for leaky-wave antennas.

A. One-dimensional glide-symmetric structures

The first studies on the dispersion of glide-symmetric structures were done in one-dimensional periodic structures [5]. When the coupling between sub-unit cells is strong, the dispersion of the modes propagating in the new periodic structure is reduced. More recently, these results were corroborated for thin metallic corrugations [8], planar bifilar lines [50] and slotted lines [11], [12]. One example of slotted lines is represented in Fig. 2 (b). In all these studies, and for all these different technologies, when glide symmetry was applied, the first and second modes were connected, removing the first stop-band [9]. The elimination of the first stop band inherently reduces the dispersion of the first mode is reduced, which means that the the bandwidth is increased. This feature can be used to control the radiation of leaky-wave antennas [52], [12], [53].

Although the majority of the examples of glide symmetry make use of two layers to implement glide symmetry, a new type of flat glide symmetry was proposed in [51]. In this work, elliptical holes were introduced between two dielectric layers. These holes modify the propagation characteristics of the parallel plate modes inside each layer, and glide symmetry can be used to reduce their dispersion.

B. Two-dimensional glide-symmetric structures

Similarly to one-dimensional periodic structures, two-dimensional glide-symmetric structures are less dispersive than the conventional one. In [15], it has been demonstrated that fully-metallic glide-symmetric structures reduce the dispersion of the first propagating modes in PPW. Additionally, the first mode is able to produce higher refractive indexes and it is more isotropic. This technique was employed to produce a broadband Luneburg lens in [54] with holey structures in Ka-band. A photo of this lens is plotted in Fig. 5 (a), and its radiation patterns at 28 GHz in Fig. 5 (b).

Although the first implementations of two-dimensional glide-symmetric structures were based on holey structures, similar properties were also found for glide-symmetric pins [55], [56], [57]. Both, pins and holes, can be implemented to produce anisotropic responses. For example, rectangular holes were studied in [16], and elliptical holes in [24]. In both cases, anisotropy was achieved without affecting the broadband response of the unit cells. These anisotropic unit cells can be used to compress the size of lenses with transformation optics [58], which is in asset in practical applications [6].

Another example of two-dimensional glide symmetry can be found in [59]. In this work, the authors demonstrated that nearby layers of patches that possess glide symmetry are able to produce high equivalent refractive indexes. Similarly to this work, glide symmetry demonstrated to be a good candidate to produce dense materials which can be used for lens antennas [60], [61].
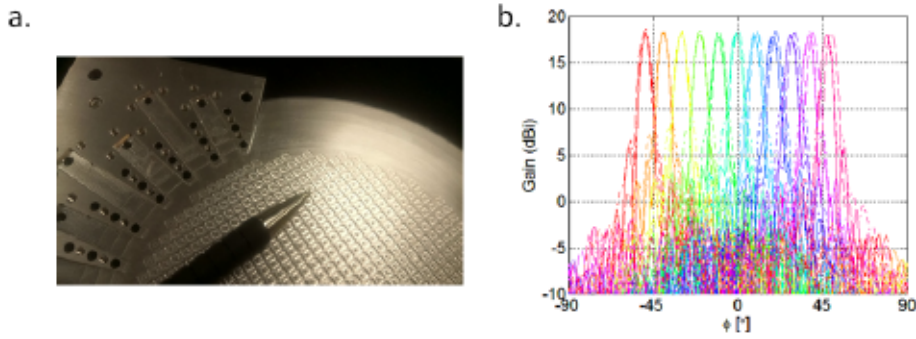
Fig. 5. Glide-symmetric Luneburg lens [54]: a) Photo of a glide-symmetric Luneburg lens. b) Radiation Pattern at 28 GHz.

Other recent implementations of two-dimensional glide-symmetric structures include multi-layer glide-symmetric metasurfaces [62], [63], dielectric lenses as in [64], reconfigurable planar lenses in the optical regime [65] and broadband slow acoustic waves [66].

VIII. TWIST-SYMMETRIC STRUCTURES

As explained in Section II-B, twist symmetry is also a higher symmetry. Similar to glide symmetries, twist-symmetric structures have propagation properties which differ from common periodic structures [67]. They can be also described with analogous models to glide symmetry. In [5], it was demonstrated that an m-fold twist line leads to the suppression of the first $m-1$ stop-bands in its Brillouin diagram. As in glide-symmmetric structures, this effect can be used to reduce the frequency dispersion.

Following the generalized Floquet theorem, m-fold twist-symmetric structures can be characterized by a sub-unit cell of length p/m. Therefore, they can be analyzed with equivalent-circuit models as in IV-A [14] and with a multi-modal approach similar to the one described in Section IV-B [21]. The latter method requires to describe a sub-unit cell as a $2N$-port network, where N is the number of background modes retained at each Floquet boundary, and define a sub-cell transmission matrix $\boldsymbol{T}_{1/m}$ as in (2). In glide structures we defined a set of even and odd modes with respect to the glide plane, and this parity was responsible to the sign of the relevant voltage and current in the right-hand side of (2). In twist structures, the modes can be classed according to their azimuthal variation on the circular cross section of the waveguide ($\cos(n\varphi)$ and $\sin(n\varphi)$, for a nth azimuthal order. The modes are then rotated an angle π/m by means of a rotation matrix every translation of p/m. The eigenvalue problem in (1) can be formulated as [21]:

$$\begin{bmatrix} Q & 0 \\ 0 & Q \end{bmatrix} \cdot \boldsymbol{T}_{1/m} \cdot \begin{bmatrix} V \\ I \end{bmatrix} = e^{\, jk_z \frac{p}{m}} \begin{bmatrix} V \\ I \end{bmatrix} \tag{9}$$

where the $\boldsymbol{Q}$ matrix rotates the background mode at the sub-unit cell ports:

$$\boldsymbol{Q} = \begin{bmatrix} 1 & 0 & \cdots & \cdots & \cdots & \cdots & 0 \\ 0 & \ddots & \ddots & \ddots & \cdots & \cdots & \vdots \\ \vdots & \ddots & \cos\left(\frac{\pi m}{m}\right) & -\sin\left(\frac{\pi m}{m}\right) & \cdots & \cdots & \vdots \\ \vdots & \ddots & \sin\left(\frac{\pi n}{m}\right) & \cos\left(\frac{\pi n}{m}\right) & \cdots & \cdots & \vdots \\ \vdots & \ddots & \ddots & \ddots & \ddots & 0 & 0 \\ \vdots & \ddots & \ddots & \ddots & 0 & \cos\left(\frac{\pi N}{m}\right) & -\sin\left(\frac{\pi N}{m}\right) \\ 0 & \cdots & \cdots & \cdots & 0 & \sin\left(\frac{\pi N}{m}\right) & \cos\left(\frac{\pi N}{m}\right) \end{bmatrix} \tag{10}$$

where we assume that the th mode is of th azimuthal order. Here again, the presence of higher-order modes leads to a different dispersive behavior with respect to a line without a twist operation where the $\boldsymbol{Q}$ matrix would not appear in (9).

A. Symmetries in circular-section coaxial cables

Twist symmetry can be used in coaxial lines to increase their density over a large bandwidth of operation [7], [13]. Two examples of fully-metallic pin-loaded coaxial cables are illustrated in [7] (see also Fig. 6). These loads are used to increase the density of the line. Alternatively, the density can be modified with holes tailored in the inner or outer conductor [13]. If these obstacles are rotated around the axis of periodicity, the structure possesses twist symmetry. Twist symmetry reduces the dispersion of the propagating modes in these loaded lines [7], [14], [13].
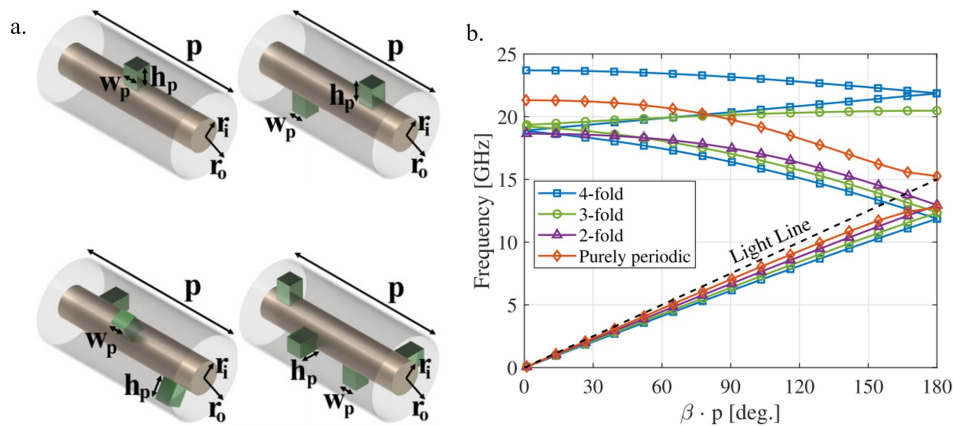

Fig. 6. a) A coaxial cable loaded with a periodic array of pin compared with 1-, 2-, 3-, and 4-fold twist symmetric configurations. b) Dispersion diagrams of the different coaxial cables as in [67].

The case of the metallic pins is discussed in [7], where the effective density of the medium is shown to be dependent on the order of the twist symmetry. Holes drilled in the inner conductor of the coaxial cable also lead to the same effect, as demonstrated experimentally in [13]. In [13], to increase the effect of the holes in the line, they were chosen to have an opening of radians. Additionally, by increasing the density of holes per unit length, the density of the line increases. The density

can be further increased by the use of twist symmetry. In [14], -radian rings were added to the outer conductor in a twist configuration, and an extension of the non-dispersive range of frequency is clearly observed when the twist order increases.

As in glide structures, the physical parameters of the scatterers along the line can be easily changed, thus obtaining a graded-index line [13], where different frequencies can be rejected at different positions of the transmission line.

In circular coaxial cables, another kind of symmetry can be introduced in analogy with the glide operator: the *polar glide* symmetry. This symmetry is created by translating half a period the obstacle in one conductor and mirroring into the other conductor [7], [13], [14]. This operation is not rigorously a glide symmetry, and then does not close the first stop-band at the edge of the Brillouin zone. However, a fine tuning of the structure can lead in waveguide with circular cross section to similar effects as the glide symmetry in Cartesian coordinates. Polar glide -radian rings were employed in [13] to prove this effect. In [14], a polar glide was implemented with -radian rings, which are equivalent to a stepped discontinuity in the conductor radius. In its polar glide configuration, this stepped discontinuity alternates between the inner and the outer conductor radii. This geometry can be described with an accurate circuit model made of the cascade of coaxial cables with different cross sections and the coupling between elements.

Another original way to combine twist and glide symmetries was proposed in [68], where an helicoidal radiating line (i.e., an helix antenna) is perturbed with periodic corrugations. A sequence of periodic corrugations naturally defines a twist symmetry due to the helicoidal shape of the line. Furthermore, a glide-symmetric sequence of corrugations can also be combined with the twist symmetry of the line. As a result, several geometric parameters can be used to tune the propagation features along the line with a broadband response. In turn, in [68], it was proved that an helix antenna can be miniaturized without deteriorating its performance.

B. Twist-symmetric waveguides and metasurfaces

Twist symmetries can also be implemented in circular waveguides, as shown in [69] (see Fig. 7). In this work, a waveguide was periodically loaded with metallic-sheets with perforated holes of circular shape that are not centered in the waveguide cross-section. These obstacles block the usual TE propagation and let only TM modes propagate in the waveguide. Furthermore, if these circular holes are rotated in a twist symmetric feature, the stop-bands between the first modes are suppressed. Acting on geometrical parameters, a broader band of propagation is available as the period decreases, thus leading to a miniaturization of the line. Finally, if the holes have an elliptical shape, their twist-symmetric rotation opens a pass-band (Fig. 7(a)), while different kinds of rotations of the same obstacles keep the structure in stop-band (Fig. 7(b)).

Other applications of twist symmetry can be encountered in metasurface design. For example, in [70], a multilayered configuration of metasurfaces based on split-ring resonators was proposed. The layered structure is locally twist-symmetric with respect to the stratification direction (Fig. 8). The electric density seen by a plane wave traveling across the metasurfaces is shown to depend on the twist order. This leads to the design of a flat lens illuminated by a spherical wave, providing different phase delays at each incidence point. These delays were designed to obtain a plane wave emerging from the lens. The design maintained the orientation of the split rings on the first and the last metasurfaces, so that no depolarization is encountered.
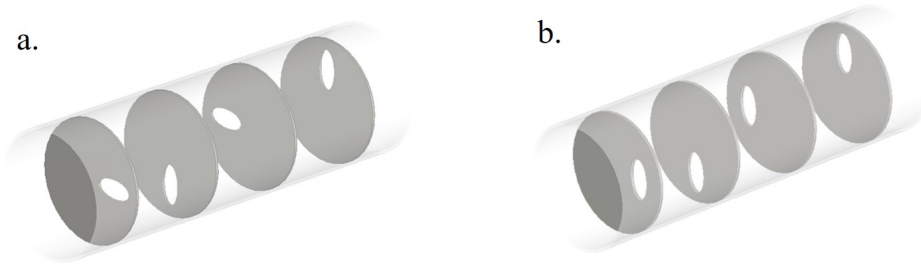
Fig. 7. a) Circular waveguide with twist-symmetric irises as in [69]. b) Non-twist-symmetric circular waveguide whose irises are not rotated according to the twist-operator definition.

However, a different configuration can be easily designed in order to obtain a given polarization conversion [71], [72], [73], [74].
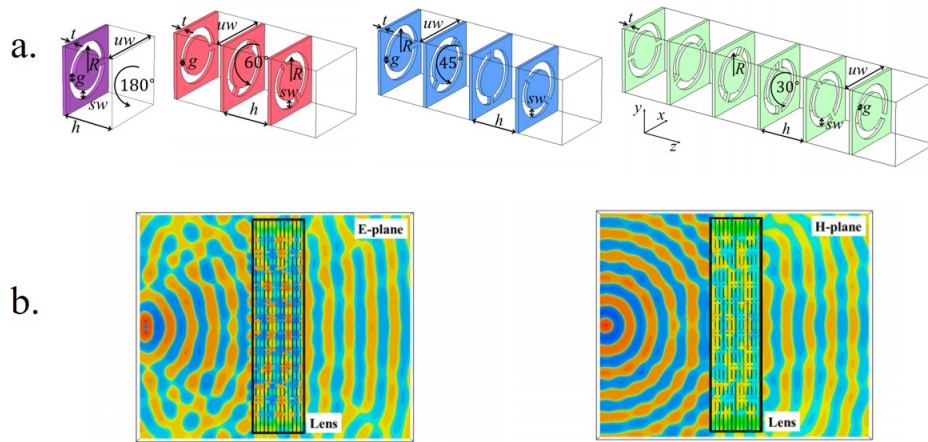

Fig. 8. a) Twist unit cells achieving different electrical density according to the twist order, with respect to a wave impinging along the direction of stratification. b) Lens focusing a spherical wave into a plane wave on both principal planes, realized with the unit cells in (a). Figure from [70].

IX. CONCLUSION

In this paper, we have described the latest discoveries on higher symmetries and their opportunities for designing electromagnetic devices. There are two known types of spatial higher symmetries: glide and twist. Glide symmetry has been the most broadly studied, since it can be implemented in planar structures, which are easy to manufacture.

For example, glide symmetry has been proposed to reduce the dispersion properties of the first propagating mode in parallel plate configurations. This opened possibilities to increase the bandwidth of metasurface lens antennas and leaky-wave antennas.

Additionally, glide symmetry was reported to increase the bandwidth of operation of conventional EBGs. This opened opportunities, for example, for cost-effective and robust gap waveguide technology.

Glide symmetry has been also proposed to produce tunable stop-bands and to increase the bandwidth of filters. Finally, in more recent works, glide symmetry was found suitable for dielectric configurations and optical applications.

On the other hand, twist symmetries have been less studied than glide symmetries due to the complexity of their practical implementation. Similarly to glide symmetries, they have been proposed to reduce the dispersion of propagating modes, and to control stop-bands in transmission lines, waveguides and flat metasurfaces.

R E F E R E N C E S

[1] G. L. Trigg, "Higher symmetries," *Physical Review Letters*, vol. 14, pp. 479–479, Mar 1965.

[2] P. J. Crepeau and P. R. McIsaac, "Consequences of symmetry in periodic structures," *Proceedings of the IEEE*, vol. 52, no. 1, pp. 33–43, Jan 1964.

[3] R. Mittra and S. Laxpati, "Propagation in a wave guide with glide reflection symmetry," *Canadian Journal of Physics*, vol. 43, no. 2, pp. 353–372, 1965.

[4] R. Kieburtz and J. Impagliazzo, "Multimode propagation on radiating traveling-wave structures with glide-symmetric excitation," *IEEE Transactions on Antennas and Propagation*, vol. 18, no. 1, pp. 3–7, Jan 1970.

[5] A. Hessel, M. H. Chen, R. C. M. Li, and A. A. Oliner, "Propagation in periodically loaded waveguides with higher symmetries," *Proceedings of the IEEE*, vol. 61, no. 2, pp. 183–195, Feb 1973.

[6] O. Quevedo-Teruel, M. Ebrahimpouri, and F. Ghasemifard, "Lens antennas for 5G communications systems," *IEEE Communications Magazine*, vol. 56, no. 7, pp. 36–41, July 2018.

[7] O. Dahlberg, R. C. Mitchell-Thomas, and O. Quevedo-Teruel, "Reducing the dispersion of periodic structures with twist and polar glide symmetries," *Scientific Reports*, vol. 7, no. 1, p. 10136, 8 2017.

[8] R. Quesada, D. Martín-Cano, F. J. García-Vidal, and J. Bravo-Abad, "Deep-subwavelength negative-index waveguiding enabled by coupled conformal surface plasmons," *Optics Letters*, vol. 39, no. 10, pp. 2990–2993, May 2014.

[9] G. Valerio, Z. Sipus, A. Grbic, and O. Quevedo-Teruel, "Accurate equivalent-circuit descriptions of thin glide-symmetric corrugated metasurfaces," *IEEE Transactions on Antennas and Propagation*, vol. 65, no. 5, pp. 2695–2700, May 2017.

[10] F. Ghasemifard, M. Norgren, and O. Quevedo-Teruel, "Dispersion analysis of 2-D glide-symmetric corrugated metasurfaces using mode-matching technique," *IEEE Microwave and Wireless Components Letters*, vol. 28, no. 1, pp. 1–3, Jan 2018.

[11] M. Camacho, R. C. Mitchell-Thomas, A. P. Hibbins, J. R. Sambles, and O. Quevedo-Teruel, "Designer surface plasmon dispersion on a one-dimensional periodic slot metasurface with glide symmetry," *Optics Letters*, vol. 42, no. 17, pp. 3375–3378, Sep 2017.

[12] ——, "Mimicking glide symmetry dispersion with coupled slot metasurfaces," *Applied Physics Letters*, vol. 111, no. 12, p. 121603, 2017.

[13] F. Ghasemifard, M. Norgren, and O. Quevedo-Teruel, "Twist and polar glide symmetries: an additional degree of freedom to control the propagation characteristics of periodic structures," *Scientific Reports*, vol. 8, no. 11266, July 2018.

[14] Q. Chen, F. Ghasemifard, G. Valerio, and O. Quevedo-Teruel, "Modeling and dispersion analysis of coaxial lines with higher symmetries," *IEEE Transactions on Microwave Theory and Techniques*, vol. 66, no. 10, pp. 4338–4345, Oct 2018.

[15] O. Quevedo-Teruel, M. Ebrahimpouri, and M. N. M. Kehn, "Ultrawideband metasurface lenses based on off-shifted opposite layers," *IEEE Antennas and Wireless Propagation Letters*, vol. 15, pp. 484–487, Dec 2016.

[16] G. Valerio, F. Ghasemifard, Z. Sipus, and O. Quevedo-Teruel, "Glide-symmetric all-metal holey metasurfaces for low-dispersive artificial materials: Modeling and properties," *IEEE Transactions on Microwave Theory and Techniques*, vol. 66, no. 7, pp. 3210–3223, July 2018.

[17] F. Ghasemifard, M. Norgren, O. Quevedo-Teruel, and G. Valerio, "Analyzing glide-symmetric holey metasurfaces using a generalized Floquet theorem," *IEEE Access*, vol. 6, pp. 71 743–71 750, 2018.

[18] S. Sensiper, "Electromagnetic wave propagation on helical structures (a review and survey of recent progress)," *Proceedings of the IRE*, vol. 43, no. 2, pp. 149–161, Feb 1955.

[19] M. Bagheriasl, O. Quevedo-Teruel, and G. Valerio, "Bloch analysis of artificial lines and surfaces exhibiting glide symmetry," *IEEE Transactions on Microwave Theory and Techniques*, vol. 67, no. 7, July 2019.

[20] F. Mesa, R. Rodríguez-Berral, and F. Medina, "On the computation of the dispersion diagram of symmetric one-dimensionally periodic structures," *Symmetry*, vol. 10, no. 8, 2018.

[21] M. Bagheriasl and G. Valerio, "Bloch analysis of electromagnetic waves in twist-symmetric lines," *Symmetry*, vol. 5, no. 1, p. 620, 2019.

[22] N. Marcuvitz, *Waveguide Handbook*. Isha Books, 2013.

[23] B. A. Mouris, A. Fernandez-Prieto, R. Thobaben, J. Martel, F. Mesa, and O. Quevedo-Teruel, "On the increment of the bandwidth of mushroom-type EBG structures with glide symmetry," *submitted to IEEE Transactions on Microwave Theory Technology*.

[24] A. Alex-Amor, F. Ghasemifard, G. Valerio, P. Padilla, J. M. Fernandez-Gonzalez, and O. Quevedo-Teruel, "Glide-symmetric metallic structures with elliptical holes," *submitted to IEEE Transactions on Microwave Theory and Techniques*.

[25] F. J. Garcia-Vidal, L. Martin-Moreno, and J. B. Pendry, "Surfaces with holes in them: New plasmonic metamaterials," *Journal of Optics A: Pure and Applied Optics*, vol. 7, pp. S97–S101, 2005.

[26] F. J. García de Abajo and J. J. Sáenz, "Electromagnetic surface modes in structured perfect-conductor surfaces," *Physical Review Letters*, vol. 95, p. 233901, Nov 2005.

[27] G. Valerio, Z. Sipus, A. Grbic, and O. Quevedo-Teruel, "Nonresonant modes in plasmonic holey metasurfaces for the design of artificial flat lenses," *Optics Letters*, vol. 42, no. 10, pp. 2026–2029, May 2017.

[28] S. T. Peng, T. Tamir, and H. L. Bertoni, "Theory of periodic dielectric waveguides," *IEEE Transactions on Microwave Theory and Techniques*, vol. 23, pp. 123–133, 1975.

[29] Z. Sipus and M. Bosiljevac, "Modelling of glide-symmetric dielectric structures," *Symmetry*, vol. 11, 2019.

[30] D. Sievenpiper, Lijun Zhang, R. F. J. Broas, N. G. Alexopolous, and E. Yablonovitch, "High-impedance electromagnetic surfaces with a forbidden frequency band," *IEEE Transactions on Microwave Theory and Techniques*, vol. 47, no. 11, pp. 2059–2074, Nov 1999.

[31] O. Quevedo-Teruel, L. Inclan-Sanchez, and E. Rajo-Iglesias, "Soft surfaces for reducing mutual coupling between loaded pifa antennas," *IEEE Antennas and Wireless Propagation Letters*, vol. 9, pp. 91–94, 2010.

[32] L. Inclan-Sanchez, J. Vazquez-Roy, and E. Rajo-Iglesias, "High isolation proximity coupled multilayer patch antenna for dual-frequency operation," *IEEE Transactions on Antennas and Propagation*, vol. 56, no. 4, pp. 1180–1183, April 2008.

[33] P. Kildal, E. Alfonso, A. Valero-Nogueira, and E. Rajo-Iglesias, "Local metamaterial-based waveguides in gaps between parallel metal plates," *IEEE Antennas and Wireless Propagation Letters*, vol. 8, pp. 84–87, 2009.

[34] P. . Kildal, A. U. Zaman, E. Rajo-Iglesias, E. Alfonso, and A. Valero-Nogueira, "Design and experimental verification of ridge gap waveguide in bed of nails for parallel-plate mode suppression," *IET Microwaves, Antennas Propagation*, vol. 5, no. 3, pp. 262–270, Feb 2011.

[35] E. Rajo-Iglesias and P. Kildal, "Groove gap waveguide: A rectangular waveguide between contactless metal plates enabled by parallel-plate cut-off," in *Proceedings of the Fourth European Conference on Antennas and Propagation*, April 2010.

[36] D. Dawn, Y. Ohashi, and T. Shimura, "A novel electromagnetic bandgap metal plate for parallel plate mode suppression in shielded structures," *IEEE Microwave and Wireless Components Letters*, vol. 12, no. 5, pp. 166–168, May 2002.

[37] M. Ebrahimpouri, O. Quevedo-Teruel, and E. Rajo-Iglesias, "Design guidelines for gap waveguide technology based on glide-symmetric holey structures," *IEEE Microwave and Wireless Components Letters*, vol. 27, no. 6, pp. 542–544, June 2017.

[38] M. Ebrahimpouri, E. Rajo-Iglesias, Z. Sipus, and O. Quevedo-Teruel, "Low-cost metasurface using glide symmetry for integrated waveguides," in *2016 10th European Conference on Antennas and Propagation (EuCAP)*, April 2016, pp. 1–2.

[39] ——, "Cost-effective gap waveguide technology based on glide-symmetric holey EBG structures," *IEEE Transactions on Microwave Theory and Techniques*, vol. 66, no. 2, pp. 927–934, Feb 2018.

[40] E. Rajo-Iglesias, M. Ebrahimpouri, and O. Quevedo-Teruel, "Wideband phase shifter in groove gap waveguide technology implemented with glide-symmetric holey EBG," *IEEE Microwave and Wireless Components Letters*, vol. 28, no. 6, pp. 476–478, June 2018.

[41] P. Padilla, A. Palomares-Caballero, A. Alex-Amor, J. Valenzuela-Valdés, J. M. Fernández-González, and O. Quevedo-Teruel, "Broken glide-symmetric holey structures for bandgap selection in gap-waveguide technology," *IEEE Microwave and Wireless Components Letters*, vol. 29, no. 5, pp. 327–329, May 2019.

[42] A. Palomares-Caballero, A. Alex-Amor, P. Padilla, F. Luna, and J. Valenzuela-Valdes, "Compact and low-loss v-band waveguide phase shifter based on glide-symmetric pin configuration," *IEEE Access*, vol. 7, pp. 31 297–31 304, 2019.

[43] M. Ebrahimpouri, A. A. Brazalez, L. Manholm, and O. Quevedo-Teruel, "Using glide-symmetric holes to reduce leakage between waveguide flanges," *IEEE Microwave and Wireless Components Letters*, vol. 28, no. 6, pp. 473–475, June 2018.

[44] E. Rajo-Iglesias and P. . Kildal, "Numerical studies of bandwidth of parallel-plate cut-off realised by a bed of nails, corrugations and mushroom-type electromagnetic bandgap for use in gap waveguides," *IET Microwaves, Antennas Propagation*, vol. 5, no. 3, pp. 282–289, Feb 2011.

[45] Q. Liao, E. Rajo-Iglesias, and O. Quevedo-Teruel, "Ka-band fully metallic TE$_{40}$ slot array antenna with glide-symmetric gap waveguide technology," *IEEE Transactions on Antennas and Propagation, in press*.

[46] A. Palomares-Caballero, A. Alex-Amor, J. Valenzuela-Valdes, and P. Padilla, "Millimeter-wave gap-waveguide 3D-printed antenna array based on glide-symmetric holey structures," *submitted to IEEE Transactions on Antennas and Propagation*.

[47] A. Vosoogh, H. Zirath, and Z. S. He, "Novel air-filled waveguide transmission line based on multilayer thin metal plates," *IEEE Transactions on Terahertz Science and Technology*, vol. 9, no. 3, pp. 282–290, May 2019.

[48] S. Rahiminejad, E. Pucci, V. Vassilev, P. Kildal, S. Haasl, and P. Enoksson, "Polymer gap adapter for contactless, robust, and fast measurements at 220–325 GHz," *Journal of Microelectromechanical Systems*, vol. 25, no. 1, pp. 160–169, Feb 2016.

[49] B. A. Mouris, O. Quevedo-Teruel, and R. Thobaben, "Exploiting glide symmetry in planar EBG structures," *Journal of Physics: Conference Series*, vol. 963, p. 012002, feb 2018.

[50] P. Padilla, L. F. Herrán, A. Tamayo-Domínguez, J. F. Valenzuela-Valdés, and O. Quevedo-Teruel, "Glide symmetry to prevent the lowest stopband of printed corrugated transmission lines," *IEEE Microwave and Wireless Components Letters*, vol. 28, no. 9, pp. 750–752, Sep. 2018.

[51] A. Tamayo-Dominguez, J.-M. Fernandez-Gonzalez, and O. Quevedo-Teruel, "One-plane glide-symmetric holey structures for stop-band and refraction index reconfiguration," *Symmetry*, vol. 11, no. 4, 2019.

[52] J. J. Wu, C. Wu, D. J. Hou, K. Liu, and T. Yang, "Propagation of low-frequency spoof surface plasmon polaritons in a bilateral cross-metal diaphragm channel waveguide in the absence of bandgap," *IEEE Photonics Journal*, vol. 7, no. 1, pp. 1–8, Feb 2015.

[53] Q. Chen, O. Dahlberg, E. Pucci, A. Palomares-Caballero, P. Padilla, and O. Quevedo-Teruel, "Glide-symmetric holey leaky-wave antenna with low dispersion for 60-GHz point-to-point communications," *submitted to IEEE Transactions on Antennas and Propagation*.

[54] O. Quevedo-Teruel, J. Miao, M. Mattsson, A. Algaba-Brazalez, M. Johansson, and L. Manholm, "Glide-symmetric fully metallic luneburg lens for 5G communications at Ka-band," *IEEE Antennas and Wireless Propagation Letters*, vol. 17, no. 9, pp. 1588–1592, Sept 2018.

[55] K. Liu, F. Ghasemifard, and O. Quevedo-Teruel, "Broadband metasurface luneburg lens antenna based on glide-symmetric bed of nails," in *2017 11th European Conference on Antennas and Propagation (EUCAP)*, March 2017, pp. 358–360.

[56] N. Memeletzoglou, C. Sanchez-Cabello, F. Pizarro-Torres, and E. Rajo-Iglesias, "Analysis of periodic structures made of pins inside a parallel plate waveguide," *Symmetry*, vol. 11, no. 4, 2019.

[57] D. Sun, X. Chen, J. Deng, L. Guo, W. Cui, K. Yin, Z. Chen, C. Yao, and F. Huang, "Gap waveguide with interdigital-pin bed of nails for high-frequency applications," *IEEE Transactions on Microwave Theory and Techniques*, 2019.

[58] M. Ebrahimpouri and O. Quevedo-Teruel, "Ultra-wideband anisotropic glide-symmetric metasurfaces," *IEEE Antennas and Wireless Propagation Letters, in press*.

[59] T. Chang, J. U. Kim, S. K. Kang, H. Kim, D. K. Kim, Y.-H. Lee, and J. Shin, "Broadband giant-refractive-index material based on mesoscopic space-filling curves," *Nature Communications*, vol. 7, Article number 12661, 2016.

[60] D. Cavallo and C. Felita, "Analytical formulas for artificial dielectrics with nonaligned layers," *IEEE Transactions on Antennas and Propagation*, vol. 65, no. 10, pp. 5303–5311, Oct 2017.

[61] D. Cavallo, "Dissipation losses in artificial dielectric layers," *IEEE Transactions on Antennas and Propagation*, vol. 66, no. 12, pp. 7460–7465, Dec 2018.

[62] J. D. de Pineda, R. C. Mitchell-Thomas, A. P. Hibbins, and J. R. Sambles, "A broadband metasurface luneburg lens for microwave surface waves," *Applied Physics Letters*, vol. 111, no. 21, p. 211603, 2017.

[63] J. D. de Pineda, A. P. Hibbins, and J. R. Sambles, "Microwave edge modes on a metasurface with glide symmetry," *Physical Review B*, vol. 98, p. 205426, Nov 2018.

[64] D. Jia, Y. He, N. Ding, J. Zhou, B. Du, and W. Zhang, "Beam-steering flat lens antenna based on multilayer gradient index metamaterials," *IEEE Antennas and Wireless Propagation Letters*, vol. 17, no. 8, pp. 1510–1514, Aug 2018.

[65] M. M. Shanei, D. Fathi, F. Ghasemifard, and O. Quevedo-Teruel, "All-silicon reconfigurable metasurfaces for multifunction and tunable performance at optical frequencies based on glide symmetry," *submitted to Scientific Reports*.

[66] J. G. Beadle, I. R. Hooper, J. R. Sambles, and A. P. Hibbins, "Broadband, slow sound on a glide-symmetric meander-channel surface," *The Journal of the Acoustical Society of America*, vol. 145, no. 5, pp. 3190–3194, 2019.

[67] O. Dahlberg, F. Ghasemifard, G. Valerio, and O. Quevedo-Teruel, "Propagation characteristics of periodic structures possessing twist and polar glide symmetries," *EPJ Applied Metamaterials*, vol. 6, p. 14, 2019.

[68] A. Palomares-Caballero, P. Padilla, A. Alex-Amor, J. Valenzuela-Valdés, and O. Quevedo-Teruel, "Twist and glide symmetries for helix antenna design and miniaturization," *Symmetry*, vol. 11, no. 3, 2019.

[69] O. Quevedo-Teruel, O. Dahlberg, and G. Valerio, "Propagation in waveguides with transversal twist-symmetric holey metallic plates," *IEEE Microwave and Wireless Components Letters*, vol. 28, no. 10, pp. 858–860, Oct 2018.

[70] O. Dahlberg, G. Valerio, and O. Quevedo-Teruel, "Fully metallic flat lens based on locally twist-symmetric array of complementary split-ring resonators," *Symmetry*, vol. 11, no. 4, 2019.

[71] Z. Wei, Y. Cao, Y. Fan, X. Yu, and H. Li, "Broadband polarization transformation via enhanced asymmetric transmission through arrays of twisted complementary split-ring resonators," *Applied Physics Letters*, vol. 99, no. 22, p. 221907, 2011.

[72] Y. Zhao, M. A. Belkin, and A. Alù, "Twisted optical metamaterials for planarized ultrathin broadband circular polarizers," *Nature Communications*, vol. 3, May 2012.

[73] A. N. Askarpour, Y. Zhao, and A. Alù, "Wave propagation in twisted metamaterials," *Physical Review B*, vol. 90, p. 054305, Aug 2014.

[74] Y. Zhao, A. N. Askarpour, L. Sun, J. Shi, X. Li, and A. Alù, "Chirality detection of enantiomers using twisted optical metamaterials," *Nature Communications*, vol. 8, Jan 2017.